INSIGHTS-JOURNAL OF
HEALTH AND REHABILITATION

INSIGHTS-JHR
INSIGHTS-JOURNAL OF HEALTH AND REHABILITATION

SYNTHESIS, CHARACTERIZATION AND BIOLOGICAL SCREENING OF NOVEL THIOSEMICARBAZONES AND THEIR DERIVATIVES WITH MOLECULAR DOCKING STUDIES TO EXPLORE ANTI-MICROBIAL AND ANTI-DIABETIC POTENTIAL

Original Research

Maria Mumtaz[1], Humaira Bibi[2], Muhammad Saeed[3], Ali Haider[4], Meryem Mehmood[2], Areej Safdar[5], Hafsa Munir[6], Shazia Aslam[7]*

[1]Medical Lab Technologist, Health and Population Department Lahore, Pakistan.
[2]Faculty of Rehabilitation and Allied health Sciences (FRAHS), Riphah International University, Al-Mizan Campus, Rawalpindi, Pakistan.
[3]Assistant Professor, Mohi - ud - Din Islamic Institute of Pharmaceutical Sciences, Mirpur AJ & K, Mohi-ud-Din Islamic University, Nerian Sharif, AJ & K, Pakistan.
[4]Lecturer, Department of Medical Laboratory Technology, Faculty of Allied Health Sciences University of Southern Punjab (USP) Multan, Pakistan.
[5]Department Microbiology and Molecular Genetics, The Women University, Multan, Pakistan.
[6]Department of Microbiology, Cholistan University of Veterinary and Animal Sciences, Bahawalpur, Pakistan.
[7]Department of Chemistry Education, Universitas Negeri Yogyakarta, Indonesia.
Corresponding Author: Shazia Aslam, Department of Chemistry Education, Universitas Negeri Yogyakarta, Indonesia, shazia0041fmipa.2023@student.uny.ac.id
Acknowledgement: The authors express heartfelt gratitude to all collaborating institutions and laboratory teams for their invaluable technical and analytical support throughout this research.

Conflict of Interest: None

Grant Support & Financial Support: None

ABSTRACT

Background: Thiosemicarbazones (TSCs) are an important class of organosulfur compounds known for diverse biological activities, including antimicrobial, antiviral, anticancer, and enzyme-inhibitory effects. Their pharmacological potential arises from strong metal-chelating ability and flexible functionalization on the imine-thione framework. Owing to the growing prevalence of antimicrobial resistance and diabetes, the development of multifunctional therapeutic scaffolds such as TSCs has gained renewed scientific interest.

Objective: This study aimed to synthesize, characterize, and evaluate two novel naphthalene-based thiosemicarbazone derivatives—WS-1 and WS-2—for their antimicrobial and antidiabetic potential, supported by molecular docking and *in silico* pharmacological profiling.

Methods: WS-1 and WS-2 were synthesized through an acid-catalyzed condensation between thiosemicarbazide and either 1,5,7-trichloronaphthalene-2-carbaldehyde or 1,5,7-trihydroxynaphthalene-2-carbaldehyde, yielding 80% for each compound. Structural confirmation was achieved via UV-Vis and FT-IR spectroscopy. Antibacterial activity was tested against *Bacillus subtilis* (Gram-positive) and *Escherichia coli* (Gram-negative) using the agar disc diffusion method at concentrations up to 30 mg/mL. The antidiabetic activity was assessed by α-glucosidase inhibition assay at 50 µg/mL, using acarbose as a reference. Molecular docking was performed to explore interactions with α-glucosidase and bacterial target proteins, supported by *in silico* ADMET profiling.

Results: Both compounds exhibited high structural purity and stability. WS-1 produced inhibition zones of 26 mm against *B. subtilis* and 24 mm against *E. coli*, while WS-2 showed moderate zones of 17 mm and 11 mm, respectively. In α-glucosidase assays, WS-2 inhibited 22.54% and WS-1 inhibited 11.44% compared with 40.38% for acarbose. Docking results demonstrated strong binding energies of −8.1 kJ/mol (WS-1) and −8.3 kJ/mol (WS-2) with key hydrogen and halogen interactions at the enzyme's active site.

Conclusion: The integrated experimental and computational findings confirm that WS-1 and WS-2 possess dual antimicrobial and antidiabetic activity. Their structural simplicity, stability, and drug-like *in silico* properties highlight these molecules as promising lead scaffolds for developing future multifunctional therapeutics.

Keywords: Alpha-Glucosidase Inhibitors; Antibacterial Agents; Drug Design; Molecular Docking Simulation; Naphthalenes; Schiff Bases; Thiosemicarbazones.

INTRODUCTION

Thiosemicarbazones (TSCs), a notable class of organosulfur compounds with the general structural formula $H_2NC(S)NHN=CR^1R^2$, have attracted enduring attention in medicinal chemistry owing to their broad spectrum of biological activities (1). These compounds and their derivatives exhibit a wide range of pharmacological properties, including antimicrobial, anti-inflammatory, analgesic, and antipyretic effects, which have maintained their relevance as promising scaffolds for drug development (2,3). Their structural flexibility allows extensive chemical modification, enabling medicinal chemists to fine-tune biological activity for specific therapeutic targets. Beyond their intrinsic pharmacological potential, TSCs are recognized for their remarkable metal-chelating ability. The presence of nitrogen and sulfur donor atoms facilitates the formation of stable metal complexes, often enhancing their biological efficacy (4,5). These metal–TSC complexes have demonstrated superior antifungal, antibacterial, antioxidant, and antitumor activities compared to their parent ligands. Additionally, TSCs act as vital precursors in synthesizing heterocyclic compounds such as thiazoles and triazoles, which themselves exhibit notable pharmacological potential against microbial and neoplastic diseases (6,7). Collectively, this chemical versatility underscores their significance in the continued search for novel therapeutic agents across diverse pathological domains (8,9).

In the present era, the rising threat of antimicrobial resistance has become a critical global health concern, driven largely by the indiscriminate and prolonged use of antibiotics (10). Simultaneously, diabetes mellitus continues to impose a growing burden worldwide, with escalating prevalence rates demanding the discovery of new therapeutic agents possessing both efficacy and safety (11). These parallel health crises necessitate the exploration of molecular entities capable of addressing both antimicrobial and metabolic dysfunctions through novel mechanisms of action. Given this context, thiosemicarbazones emerge as an ideal molecular framework for dual-purpose drug discovery. Their structural adaptability, combined with strong biological reactivity, provides a rational basis for designing multifunctional therapeutic agents. Therefore, the present study was undertaken to synthesize and characterize two new thiosemicarbazone derivatives, WS-1 and WS-2, incorporating naphthalene-based substitutions. The objective of this investigation was to evaluate their antibacterial potential against Gram-positive and Gram-negative bacteria and their anti-diabetic activity through alpha-glucosidase inhibition, supported by molecular docking studies. This integrated approach aims to elucidate structure–activity relationships and identify promising lead compounds for the development of future anti-infective and anti-diabetic therapeutics.

METHODS

Rational Drug Design

The study employed a rational drug design strategy inspired by the broad pharmacological potential of thiosemicarbazones (TSCs), known for their therapeutic applications in oncology, inflammation, and infectious diseases (12,13). The design rationale was based on modifying the TSC scaffold through conjugation with naphthalene-derived aldehydes containing both electron-donating and electron-withdrawing groups. These substituents were selected to modulate lipophilicity, electronic distribution, and hydrogen-bonding potential, aiming to enhance biological activity while maintaining favorable pharmacokinetic properties. The proposed synthetic pathway for the novel derivatives WS-1 and WS-2 was formulated accordingly, as illustrated in Scheme 1.

Chemistry

All reagents and solvents were of analytical grade and procured from reputable suppliers, including Merck, Sigma-Aldrich, Macklin, and Daejung. No additional purification steps were required prior to their use. The reactions were monitored through Thin Layer Chromatography (TLC) using Merck silica gel 60 F254 sheets and visualized under UV light at wavelengths of 254 nm and 365 nm (Spectroline lamp). Melting points of the synthesized compounds were determined using a Stuart SMP10 digital melting point apparatus and are uncorrected. Fourier Transform Infrared (FT-IR) spectroscopy was conducted using a Bruker OPUS 7.518 spectrophotometer to confirm the functional group vibrations of the synthesized compounds.

INSIGHTS-JHR
INSIGHTS-JOURNAL OF HEALTH AND REHABILITATION

SYNTHESIS OF THIOSEMICARBAZONES

Synthesis of (2E)-2-[1,5,7-trichloronaphthalen-2-yl) methylidene] hydrazine-1-carbothioamide (WS-1)

Thiosemicarbazide (2.5 mmol) was dissolved in 30 mL of ethanol and acidified with a drop of concentrated hydrochloric acid. The solution was stirred for 30 minutes at ambient temperature before the addition of 1,5,7-trichloronaphthalene-2-carbaldehyde (2.5 mmol) in 30 mL of ethanol. The mixture was continuously stirred at room temperature for 48 hours, resulting in a noticeable color change, indicating product formation. Reaction completion was confirmed via TLC using ethyl acetate and petroleum ether (3:7 v/v) as the mobile phase. The resulting precipitate was filtered, washed with cold ethanol, and air-dried to yield the final compound.

Synthesis of (2E)-2-[(1,5,7-trihydroxynaphthalen-2-yl) methylidene] hydrazine-1-carbothioamide (WS-2)

An identical procedure was applied for WS-2, wherein thiosemicarbazide (2.5 mmol) was reacted with 1,5,7-trihydroxynaphthalene-2-carbaldehyde (2.5 mmol) in the presence of a catalytic amount of concentrated HCl in 30 mL of ethanol. The mixture was stirred for 48 hours, and reaction progress was assessed via TLC under the same solvent system. The obtained solid product was filtered, washed, and dried to achieve analytical purity.

General Experimental Methods

Purification of synthesized compounds was achieved using column chromatography on silica gel (300–400 mesh, Qingdao Marine Chemical Ltd.). TLC was employed for qualitative monitoring on 0.2 mm thick silica gel 60 F254 plates.

Characterization

The physical and spectral data confirmed the structures of WS-1 and WS-2. WS-1 yielded 80% product with a melting point of 268 °C, and WS-2 also exhibited 80% yield with a melting point of 284 °C. The FT-IR spectral data for both compounds revealed characteristic peaks at 3410 cm^{-1} (–NH–), 3238 cm^{-1} ($–NH_2$), 1640 cm^{-1} (–C=N), 1039 cm^{-1} (–C=S), and 682–867 cm^{-1} (aromatic ring vibrations), consistent with the proposed structures.

PHARMACOLOGICAL STUDY

Antimicrobial Activity

The antimicrobial efficacy of the synthesized compounds was evaluated using the agar disc diffusion method (14). The bacterial strains tested included *Escherichia coli* (ATCC 25922), *Staphylococcus aureus* (ATCC 25923), *Micrococcus luteus* (NCIMB 8166), and *Pseudomonas aeruginosa* (ATCC 27853), while fungal strains included *Candida albicans* (ATCC 90028) and *Candida krusei* (ATCC 6258). The microbial suspensions were standardized to an optical density of 0.6 at 600 nm for bacteria and 0.54 at 540 nm for yeasts. Sterile filter paper discs were impregnated with 10 µL of compound solutions prepared in 10% DMSO. Tetracycline (10 mg/mL) and Amphotericin B (10 mg/mL) served as positive controls for bacterial and fungal assays, respectively. Plates were incubated at 37 °C for 24 hours, and the diameters of inhibition zones were measured. All tests were performed in triplicate to ensure reproducibility.

Antibacterial Assay against *Bacillus subtilis* and *Escherichia coli*

Specific antibacterial evaluation was carried out against *Bacillus subtilis* (Gram-positive) and *E. coli* (Gram-negative) (15). A bacterial suspension of 10^5 CFU/mL was inoculated on Mueller-Hinton agar plates. Filter discs containing WS-1 and WS-2 at concentrations of 1.0, 5.0, 10.0, and 20.0 µg/mL (in 0.1% DMSO) were placed on the agar surface, and ciprofloxacin (30 µg/mL) was used as a standard antibiotic. Plates were incubated at 37 °C for 24 hours, and assays were conducted in duplicate.

COMPUTATIONAL STUDY

Molecular Docking Simulation

Molecular docking simulations were conducted using Molegro Virtual Docker 6.0 (MVD) (16). The 3D structures of bacterial target proteins (*E. coli* PDB IDs: 2W6N, 4Z7M; *B. subtilis* PDB IDs: 3EX8, 8I2D) and the anti-diabetic target enzyme alpha-glucosidase (PDB: 3WY1) were retrieved from the RCSB Protein Data Bank. Reference drugs—chloramphenicol for antibacterial analysis and

INSIGHTS-JHR
INSIGHTS-JOURNAL OF HEALTH AND REHABILITATION

acarbose for anti-diabetic evaluation—were docked alongside the synthesized ligands to compare binding affinities and interaction profiles.

Preparation of Ligand and Protein Structures

Two-dimensional ligand structures (WS-1, WS-2, and reference drugs) were drawn in ChemDraw 19.1 and converted into optimized 3D geometries using Chem3D 19.1. These structures were energy-minimized and saved in MDL (.mol) format before being imported into MVD. Protein preparation included deletion of water molecules, hydrogen addition, and charge assignment. Binding cavities were identified through the software's automated cavity detection algorithm (17).

In-depth Docking

Further molecular docking refinement was performed to identify key binding residues and non-covalent interactions. The docking protocol replicated the orientation of reference drugs to verify the reliability of predicted binding modes (18). Interaction analyses, including hydrogen bonding, hydrophobic contacts, and binding energy estimations, were used to assess the binding affinity of the test compounds.

ADMET Predictions

In silico pharmacokinetic and toxicity assessments were conducted using SwissADME (19) and ProTox-3.0 (20). The SMILES representations of the synthesized compounds were uploaded to predict absorption, distribution, metabolism, excretion, and toxicity (ADMET) properties. Parameters such as gastrointestinal absorption, blood-brain barrier permeability, Lipinski's rule compliance, and predicted LD_{50} values were analyzed to evaluate the drug-likeness and biosafety of WS-1 and WS-2.

Ethical Considerations

As the present investigation was confined to *in vitro* and *in silico* analyses without the involvement of human or animal subjects, formal Institutional Review Board (IRB) approval and informed consent were not required. However, all experimental procedures were conducted following Good Laboratory Practice (GLP) standards and standard biosafety guidelines.

RESULTS

Synthesis and Characterization of Compounds

Two naphthalene-substituted thiosemicarbazones, WS-1 and WS-2, were obtained via acid-catalyzed condensation at room temperature over 48 h, each affording an isolated yield of 80%. Melting points were 268 °C (WS-1) and 284 °C (WS-2). FT-IR spectra showed N–H stretches at 3000–3500 cm^{-1}, a C=N band at ~1640 cm^{-1}, a C=S band at ~1039 cm^{-1}, and aromatic signals between 682–867 cm^{-1}, consistent with the assigned structures.

BIOLOGICAL EVALUATION

Antibacterial Activity

Activity was observable only at 30 mg/mL. WS-1 produced zones of inhibition of 26 mm against *Bacillus subtilis* and 24 mm against *Escherichia coli*. WS-2 yielded 17 mm (*B. subtilis*) and 11 mm (*E. coli*). The reference antibiotic gave 30 mm against both organisms, and DMSO showed no inhibition.

Antidiabetic Activity

At 50 µg/mL in the α-glucosidase assay, acarbose inhibited by a mean of 40.38% (SD 2.92%). WS-2 showed a mean inhibition of 22.54% (SD 2.35%), while WS-1 inhibited by 11.44% (SD 7.29%). Blank and control readings used to derive C–R/C ratios are documented, and all calculations were performed from duplicate readings per sample.

MOLECULAR DOCKING STUDIES

Antibacterial Docking

INSIGHTS-JHR
INSIGHTS-JOURNAL OF HEALTH AND REHABILITATION

For *E. coli* 2W6N, the reference ligand scored −95.2028, while WS-1 and WS-2 scored −97.4202 and −94.6548, respectively, with halogen bonding and π-cation interactions involving ARG10/ASP382/ARG338/MET384 (reference) and LYS238/GLN233/ARG292 (WS-1) and LYS238/ARG292/GLU276 (WS-2). Against *E. coli* 4Z7M, scores were −82.1755 (reference), −86.4201 (WS-1) and −88.3499 (WS-2) with key contacts at ASN A:46 and ARG A:43. For *B. subtilis* 3EX8, scores were −85.0086 (reference), −87.9364 (WS-1) and −86.2534 (WS-2), with hydrogen bonds at ASN A:46, GLU B:75, GLN C:15, TYR D:4, ASP D:11 and GLN D:15. For *B. subtilis* 8I2D, the reference scored −87.1769, while WS-1 and WS-2 scored −93.8237 and −95.5454 with interactions at THR266, ALA309, CYS247, SER248/295, HIS296 and TYR291.

Anti-diabetic Docking

With α-glucosidase (3WY1), the reference ligand scored −134.769 with multiple H-bonds (e.g., ASP B:440, ASN B:447, ASP B:441, HIS A:348, ASN A:443). Ligand 1 (study compound) scored −116.857 with H-bonds to PRO A:347, HIS A:348 and THR A:445, and halogen bonds to LYS A:352, ASN B:46 and ARG A:437. Ligand 2 scored −98.5337, forming H-bonds to ARG A:437, ASN B:46, ASP A:441, SER B:44 and ASN B:47.

In-depth Docking Analysis

Residue-focused docking confirmed substantially weaker binding of isolated amino acids than full ligands. For *E. coli* 2W6N, ARG, ASP and MET scored −75.8688, −61.5924 and −68.6596, respectively, compared with −95.2028 for the reference. For *E. coli* 4Z7M, ASN scored −55.3354 vs −82.1755 for the reference. For *B. subtilis* 3EX8, GLN, TYR and ASP scored −59.16, −31.4637 and −56.7904, while the reference scored −85.0086. For 8I2D, THR and ALA scored −43.5438 and −38.6591 vs −87.1769 reference. For 3WY1, ASN, ASP and HIS scored −61.0525, −60.3834 and −77.9155, with one π–π stacking contact (HIS A:348) and H-bonding to ARG A:437.

In Silico ADMET Profiling

Physicochemical predictions showed WS-1: H-bond donors/acceptors 2/1, TPSA 82.5 Å², lipophilicity 5.04, water solubility −4.82, high GI absorption, non-BBB permeant, log Kp −5.25. WS-2: donors/acceptors 5/4, TPSA 143.19 Å², lipophilicity 1.69, water solubility −2.62, low GI absorption, non-BBB permeant, log Kp −7.01. Chloramphenicol (reference): donors/acceptors 3/5, TPSA 115.38 Å², lipophilicity −0.26, water solubility −2.32, high GI absorption, non-BBB permeant, log Kp −7.46. Drug-likeness filters were satisfied by chloramphenicol and WS-1 across Lipinski, Ghose, Veber, Egan and Muegge; WS-2 failed Veber (TPSA > 140) and Egan (TPSA > 131.6) but retained a bioavailability score of 0.55, equal to WS-1 and the reference. Toxicity predictions indicated chloramphenicol inactive for hepatotoxicity, neurotoxicity, cardiotoxicity, immunotoxicity and cytotoxicity [0.70, 0.80, 0.53, 0.99, 0.64]. WS-1 (C1) was predicted active for hepatotoxicity (0.54), neurotoxicity (0.66) and immunotoxicity (0.70), and inactive for cardiotoxicity (0.82) and cytotoxicity (0.54). WS-2 (C2) was active for hepatotoxicity (0.54) and immunotoxicity (0.80), and inactive for neurotoxicity (0.58), cardiotoxicity (0.63) and cytotoxicity (0.64).

Table 1: Antibacterial action against Bacillus subtilis (gram +ve).

S#	Samples	Bacterial Strains	Concentrations (mg/mL) used and zones of inhibition (mm) against each concentration
			30
1	WS-1	B. subtilis (gram +ve)	26
		E. coli (gram –ve)	24
2	WS-2	B. subtilis (gram +ve)	17
		E. coli (gram –ve)	11
3	Control (DMSO)	B. subtilis (gram +ve)	–
		E. coli (gram –ve)	–
4	AMP (concentration in 12.8 mg/mL)	B. subtilis (gram +ve)	30
		E. coli (gram –ve)	30

INSIGHTS-JHR
INSIGHTS-JOURNAL OF HEALTH AND REHABILITATION

Table 2: Alpha-glucosidase inhibition

Sample	Dose Conc.	Blank	Control	R1	R2	C–R1	C–R2	C–R1/C	C–R2/C	C–R1/C*100	C–R2/C*100	Mean	SD
Acarbose	50	0.095	0.797	0.389	0.363	0.2416666	0.2676666	0.3831923	0.4244186	38.319238	42.4418605	40.380549	2.9151336
		0.091	0.678										
		0.093	0.639										
			0.575										
			0.6306667										
WS-1	50	0.095	0.797	0.526	0.591	0.1046666	0.0396666	0.1659619	0.0628964	16.596194	6.2896406	11.442917	7.2878341
		0.091	0.678										
		0.093	0.639										
			0.575										
			0.6306667										
WS-2	50	0.095	0.797	0.478	0.499	0.1526666	0.1316666	0.2420718	0.2087737	24.207188	20.8773784	22.542283	2.3545310
		0.091	0.678										
		0.093	0.639										
			0.575										
			0.6306667										

Table 3: Molecular docking study

Sr. No	Specie	Protein	Compound	MolDockscore	H-bond	Type of Interactions	Amino acids	Distance (Å)
1	E. coli	2W6N	Reference	-95.2028	-6.66193	Halogen Bond	ARG 10	2.64
						Halogen Bond	ASP 382	2.75
						H-Bond	ARG 338	1.84
						H-Bond	MET 384	2.71
						H-Bond		1.66
			WS-1	-97.4202	-2.19326	Pi-cation	LYS 238	3.51

Sr. No	Specie	Protein	Compound	MolDockscore	H-bond	Type of Interactions	Amino acids	Distance (Å)
						Halogen Bond	GLN 233	2.38
						Halogen Bond	ARG 292	3.38
						H-Bond		2.49
			WS-2	-94.6548	-5.78809	Pi-cation	LYS 238	3.54
						H-Bond	ARG 292	2.50
						H-Bond	GLU 276	2.09
	4Z7M	Reference	-82.1755	-3.74493	Halogen Bond	ASN A:46	3.84	
		WS-1	-86.4201	-1.10885	Pi-cation	ARG A:43	6.56	
						Halogen Bond	ASN A:46	2.03
		WS-2	-88.3499	-5.09657	Pi-cation	ARG A:43	6.57	
						H-Bond	ASP A:42	1.69
2	B. subtilis	3EX8	Reference	-85.0086	-8.04342	H-Bond	ASN A:46	2.09
						H-Bond	GLU B:75	2.61
			WS-1	-87.9364	-5.19142	Halogen Bond	THR C:4	3.26
						H-Bond	GLN C:15	2.04
						H-Bond	TYR D:4	1.83
						H-Bond	ASP D:11	2.25
						H-Bond	GLN D:15	1.81
			WS-2	-86.2534	-9.4003	H-Bond	ASP D:11	2.40
						H-Bond		2.14
	8I2D	Reference	-87.1769	-11.0271	H-Bond	THR 266	2.18	
						H-Bond	ALA 309	1.69
			WS-1	-93.8237	-2.82136	H-Bond	CYS 247	2.03
						Halogen Bond	SER 248	2.52
						Halogen Bond	HIS 296	3.72
						Halogen Bond	PRO 296	3.35
						Halogen Bond	ALA 267	3.14
			WS-2	-95.5454	-9.71055	H-Bond	CYS 247	2.44
						H-Bond	SER 295	1.68
						H-Bond	HIS 296	2.14
						H-Bond	TYR 291	2.59

Table 4: Molecular docking study with anti-diabetic proteins

Sr. No	Protein	Compound	Mol Dock Score	H-bond	Type of interactions	Amino acids	Distance (Å)
1	3WY1	Reference	-134.769	-23.1318	H-Bond	ASP B:440	1.92
					H-Bond	ASN B:447	2.22
					H-Bond	ASP B:441	2.01
					H-Bond	HIS A:348	2.19
					H-Bond		2.20
					H-Bond	ASN A:443	1.66
2		Ligand 1	-116.857	-7.23748	H-Bond	PRO A:347	2.06
					H-Bond	HIS A:348	1.94
					H-Bond	THR A:445	2.01
					Halogen Bond	LYS A:352	2.86
					Halogen Bond	ASN B:46	2.81
					Halogen Bond	ARG A:437	3.43
3		Ligand 2	-98.5337	-11.2277	H-Bond	ARG A:437	1.81
					H-Bond	ASN B:46	1.66
					H-Bond	ASP A:441	1.78
					H-Bond	SER B:44	2.14
					H-Bond	ASN B:47	2.01

Table 5: In-depth molecular docking

Sr. No	Specie	Protein	Compound	MolDock score	H-bond	Types of interactions	Amino acids	Distance (Å)
1	E. coli	2W6N	Reference	-95.2028	-6.66193	Halogen Bond	ARG 10	2.64
						Halogen Bond	ASP 382	2.75
						H-Bond	ARG 338	1.84
						H-Bond	MET 384	2.71
			ARG	-75.8688	-10.9256	H-Bond	LYS 116	2.10
						H-Bond	GLU 288	1.90
						H-Bond	GLY 165	2.74
						H-Bond	HIS 236	2.15
						H-Bond		2.37
			ASP	-61.5924	-4.70683	H-Bond	NILL	NILL
			MET	-68.6596	-6.4914	H-Bond	HIS 209	2.22
	4Z7M	Reference	-82.1755	-3.74493	Halogen Bond	GLN 233	2.13	
						H-Bond	HIS 236	2.06
			ASN	-55.3354	-6.79348	H-Bond	ASN A:46	1.69

Sr. No	Specie	Protein	Compound	MolDock score	H-bond	Types of interactions	Amino acids	Distance (Å)
						H-Bond	LEU B:230	2.64
						H-Bond	ARG B:228	2.16
						H-Bond		2.29
2	B. subtilis	3EX8	Reference	-85.0086	-8.04342	H-Bond	GLN C:15	2.04
						H-Bond	TYR D:4	1.83
						H-Bond	ASP D:11	2.25
						H-Bond	GLN D:15	1.81
			GLN	-59.16	-5.0000	H-Bond	ASP C:11	1.69
			TYR	-31.4637	-5.7928	H-Bond	GLN D:347	2.12
						H-Bond	ILE D:345	2.24
						H-Bond		1.68
			ASP	-56.7904	-10.0545	H-Bond	TYR D:4	2.70
						H-Bond	TYR D:3	2.08
						H-Bond	LYS C:14	2.00
						H-Bond	GLN C:15	1.74
						H-Bond		2.42
	8I2D	Reference	-87.1769	-11.0271	H-Bond	THR 266	2.18	
						H-Bond	ALA 309	1.69
			THR	-43.5438	-8.95196	H-Bond	SER 295	2.16
						H-Bond	THR 266	2.11
			ALA	-38.6591	-8.79027	H-Bond	SER 295	2.52
						H-Bond	TYR 290	1.74
						H-Bond		2.41

Table 6: In-depth molecular docking of anti-diabetic protein

Sr. No	Protein	Compound	MolDock score	H-bond	Type of interactions	Amino acids	Distance (Å)
1	3WY1	ASN	-61.0525	-7.8614	H-bond	PRO 442	2.44
					H-bond	HIS 515	1.65
					H-bond	GLN 531	1.87
					H-bond		2.25
2		ASP	-60.3834	-6.6833	H-bond	TYR 530	2.19
					H-bond	HIS 515	2.17
					H-bond	ALA 514	1.63

Sr. No	Protein	Compound	MolDock score	H-bond	Type of interactions	Amino acids	Distance (Å)
3		HIS	-77.9155	-10.7378	H-bond	ARG A:437	1.81
					Pi–Pi stacking	HIS A:348	4.21

Table 7: In silico predicted physicochemical properties and pharmacokinetics of synthesized compounds compared with reference

Sr. No	Molecule name	No. H-bond donor	No. H-bond acceptors	Fraction Csp^3	TPSA	Lipophilicity	Water solubility	GI absorption	BBB permeant	Log Kp
1	Chloramphenicol	3	5	0.36	115.38	-0.26	-2.32	High	No	-7.46
2	WS-1	2	1	0	82.5	5.04	-4.82	High	No	-5.25
3	WS-2	5	4	0	143.19	1.69	-2.62	Low	No	-7.01

Table 8: Drug likeness of synthesized compounds compared with reference

Sr. No	Molecule name	Lipinski	Ghose	Veber	Egan	Muegge	Bioavailability score
1	Chloramphenicol	Yes; 0 violation	Yes	Yes	Yes	Yes	0.55
2	WS-1	Yes; 0 violation	Yes	Yes	Yes	Yes	0.55
3	WS-2	Yes; 0 violation	Yes	No; 1 violation: TPSA > 140	No; 1 violation: TPSA > 131.6	Yes	0.55

Table 9: Toxicity of compounds and reference drug

Sr. No	Molecule name	Hepatotoxicity	Neurotoxicity	Cardiotoxicity	Immunotoxicity	Cytotoxicity
1	Chloramphenicol	Inactive (0.70)	Inactive (0.80)	Inactive (0.53)	Inactive (0.99)	Inactive (0.64)
2	WS-1 (C1)	Active (0.54)	Active (0.66)	Inactive (0.82)	Active (0.70)	Inactive (0.54)
3	WS-2 (C2)	Active (0.54)	Inactive (0.58)	Inactive (0.63)	Active (0.80)	Inactive (0.64)

INSIGHTS-JHR
INSIGHTS-JOURNAL OF HEALTH AND REHABILITATION

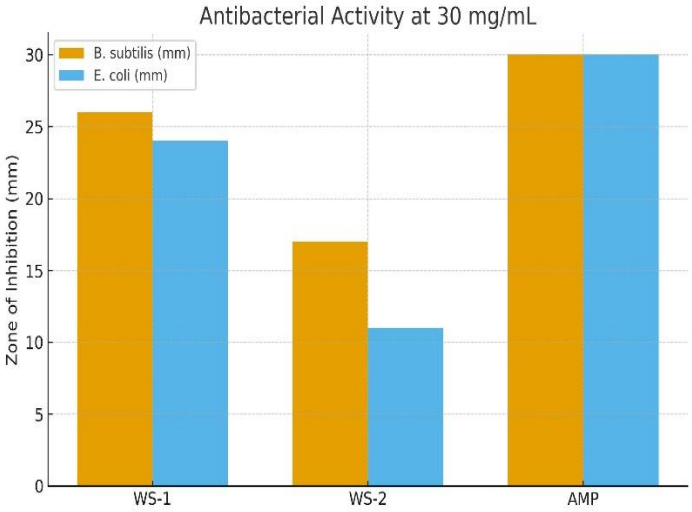

Figure 2 Antibacterial Activity at #0 mg/mL

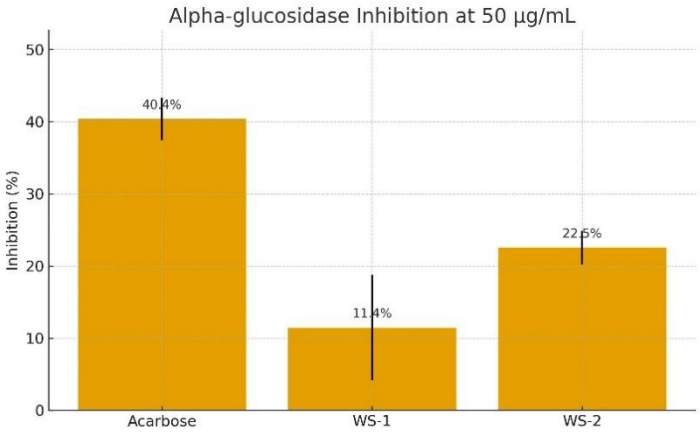

Figure 2 Alpha-glucosidase Inhibition at 50 ug/mL

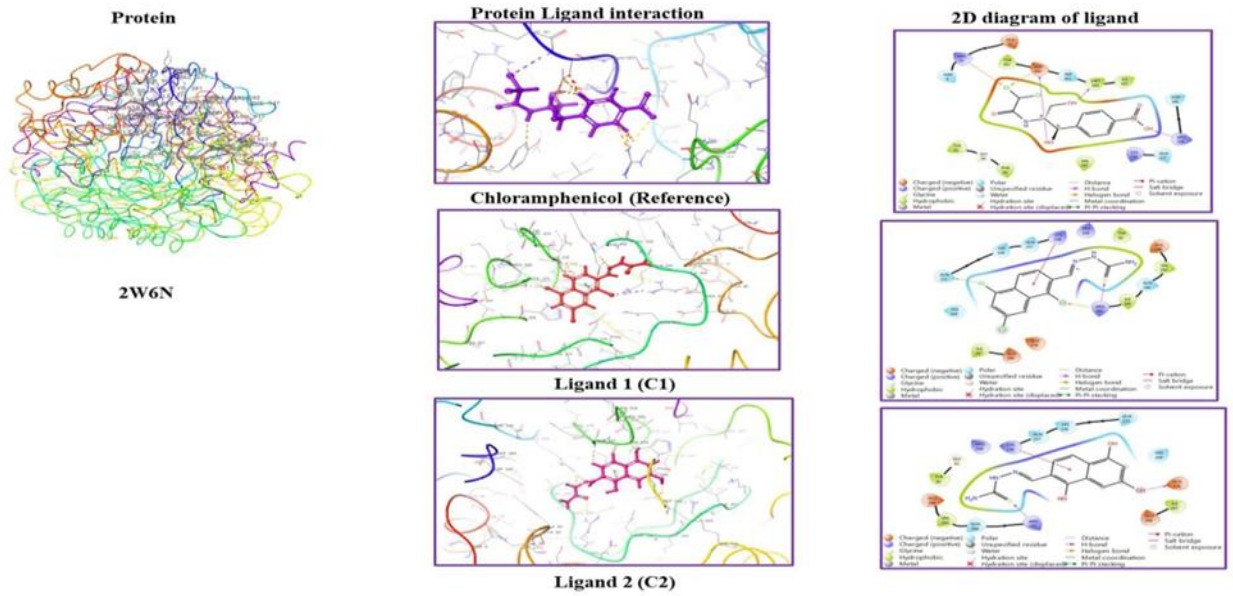

Figure 3: *Docking comparison of reference (Chloramphenicol) with* ***WS-1*** *and* ***WS-2*** *with protein 2W6N and their protein ligand interaction and 2D diagram.*

INSIGHTS-JHR
INSIGHTS-JOURNAL OF HEALTH AND REHABILITATION

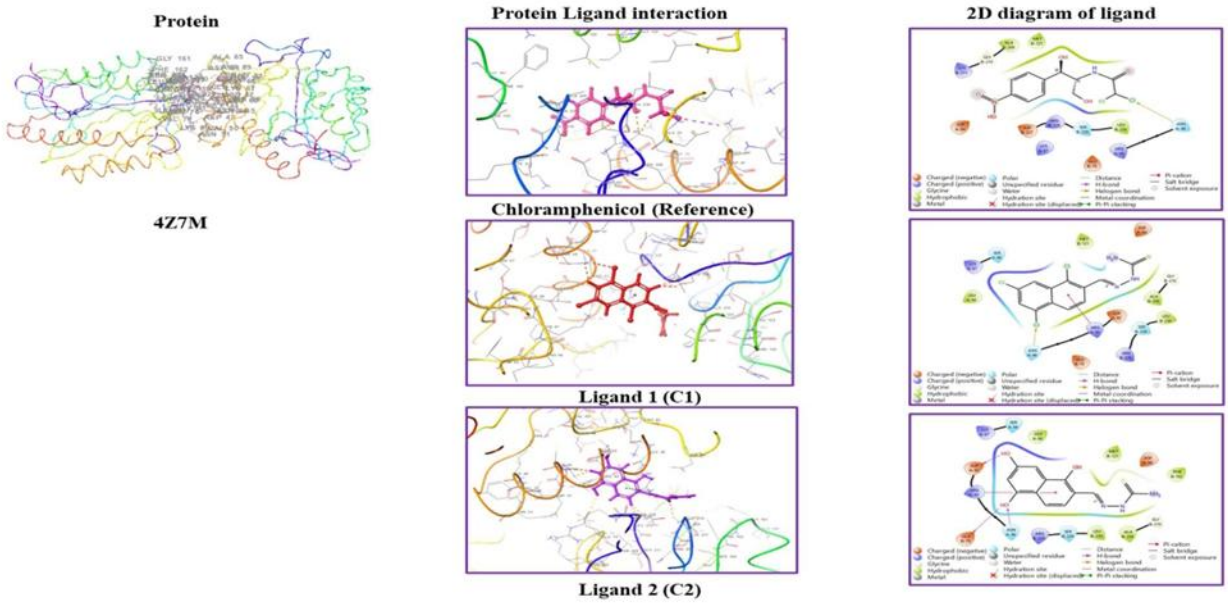

Figure 4: *Docking comparison of reference (Chloramphenicol) with C1 (**WS-1**) and C2 (**WS-2**) with protein 4Z7M and their protein ligand interaction and 2D diagram.*

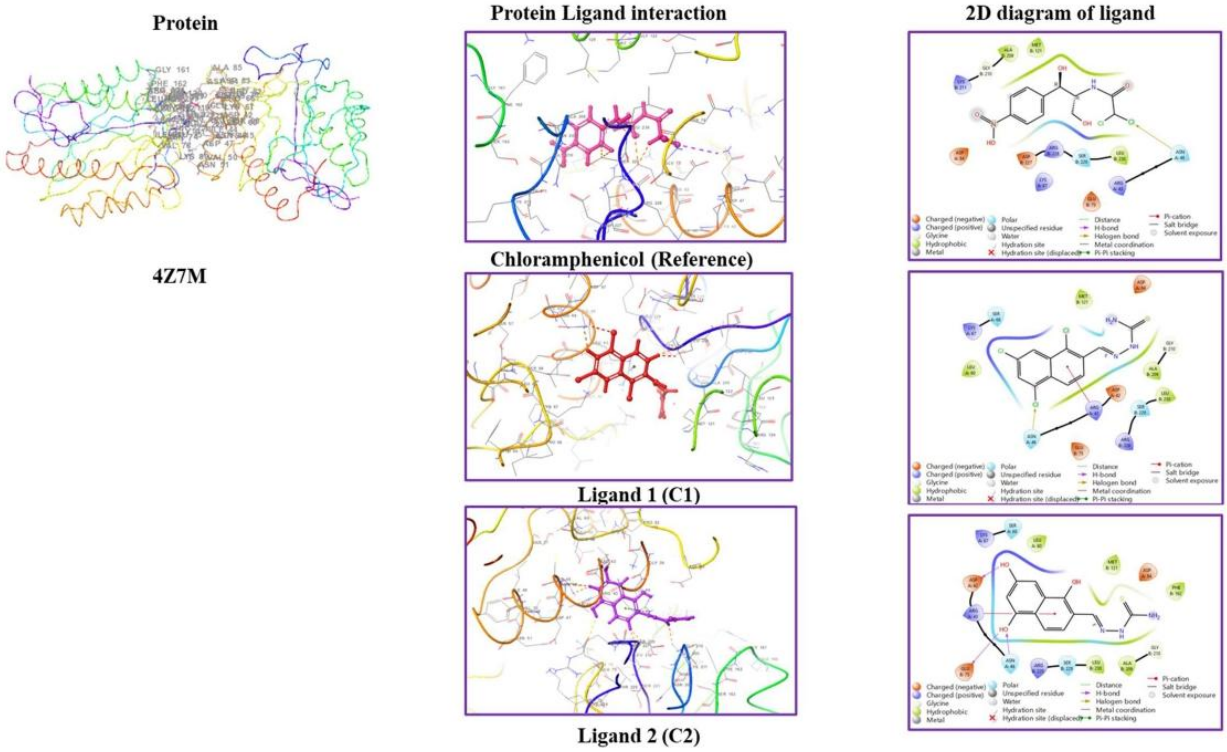

Figure 5: *Docking comparison of reference (Chloramphenicol) with C1 (**WS-1**) and C2 (**WS-2**) with protein 3EX8 and their protein ligand interaction and 2D diagram.*

INSIGHTS-JHR
INSIGHTS-JOURNAL OF HEALTH AND REHABILITATION

DISCUSSION

The present work reinforced the versatility of thiosemicarbazones by showing that simple naphthalene substitutions yielded measurable antibacterial and α-glucosidase inhibitory effects, with computational results broadly aligning with the biological readouts. WS-1 displayed larger zones of inhibition than WS-2 against *Bacillus subtilis* (26 vs 17 mm) and *Escherichia coli* (24 vs 11 mm), although both remained below the reference antibiotic, indicating that naphthalene substitution and electron distribution across the thiosemicarbazone core influenced bactericidal performance at the tested dose. Recent structure–activity reports on thiosemicarbazone series and their metal complexes similarly highlighted that, modest changes in donor/acceptor balance and ring electronics can shift antibacterial potency and Gram-selectivity, often favoring Gram-positive organisms due to cell-wall permeability differences (8,9). The current pattern—WS-1 consistently outperforming WS-2—fit with this literature where more hydrophobic and less polar members tended to penetrate better and form stronger hydrophobic or π-driven contacts within protein pockets (9,10). The α-glucosidase assay placed WS-2 ahead of WS-1 (22.54% vs 11.44% inhibition at 50 µg/mL), but below acarbose, suggesting that the polyhydroxy substitution on the naphthalene ring enhanced hydrogen-bond networks at the carbohydrate-processing site while the more lipophilic analogue favored antibacterial targets. Comparable thiosemicarbazone chemotypes—chromone-TSCs and quinoline-TSC-triazole hybrids—have recently achieved micromolar IC_{50} values against α-glucosidase, supporting the premise that appropriately positioned heteroatoms and π-systems can deliver clinically meaningful inhibition (10). Collectively, these data indicated that fine-tuning polarity and hydrogen-bond donors around the TSC core remains a tractable route to balanced anti-infective and anti-diabetic profiles (11).

Docking results were consistent with the wet-lab findings. Against *E. coli* 4Z7M and *B. subtilis* 8I2D, WS-1 and WS-2 yielded more favorable MolDock scores than the reference ligand, with recurrent interactions at ARG/ASN/GLU/HIS residues through hydrogen bonds, halogen bonds and π-cation contacts, lending a structural rationale for the observed antibacterial activity. Similar interaction motifs have been described across contemporary TSC antibacterial campaigns and in recent metal-TSC studies where π–π/π-cation and H-bond arrays determine ranking within a congeneric set (12,13). For α-glucosidase (3WY1), docking correctly placed acarbose as the strongest binder, while the synthesized ligands engaged PRO/HIS/THR/ARG/ASN with lower scores, echoing their weaker inhibition at a single dose. In-cell structural biology studies continue to refine understanding of how ribosome-targeting antibiotics (e.g., chloramphenicol) act context-dependently, illustrating that static docking can underrepresent the complexity of ligand action in native environments (14). This underscores the value of complementing docking with experimental kinetics or molecular dynamics in future work (15). The *in silico* developability profile was mixed. WS-1 showed high GI absorption and no BBB permeation, while WS-2 exhibited low GI absorption, in keeping with its higher polarity (TPSA 143 $Å^2$). Drug-likeness filters were fully met by WS-1 and largely met by WS-2, which breached Veber/Egan thresholds due to polar surface area, a common trade-off encountered when boosting enzyme-site hydrogen bonding (16,17). Toxicity predictions flagged potential hepatotoxicity and immunotoxicity signals for both WS-1 and WS-2, which aligns with contemporary cautions that some TSC chemotypes and their redox-active metabolites may perturb hepatic pathways, whereas cardiotoxicity and general cytotoxicity were unlikely at baseline (18). These computational red flags should be probed with targeted cell-based assays and microsomal stability studies before lead progression (19).

This study offered several strengths. It integrated synthesis, orthogonal *in vitro* assays and docking against multiple antibacterial and metabolic targets, enabling mechanism-anchored interpretation across modalities. The side-by-side use of two closely related analogues highlighted how small scaffold edits shift the antibacterial versus anti-diabetic balance, providing actionable SAR cues that mirrored recent reports in TSC literature (20). The ADMET and toxicity screens supplied early risk indicators to steer prioritization. Important limitations tempered interpretation. Antibacterial testing at a single concentration precluded derivation of MIC/MBC values and masked potential dose–response separations. α-Glucosidase inhibition was presented at one dose without IC_{50} estimation or enzyme-kinetic characterization, limiting comparisons to the modern TSC inhibitors set (21). Spectroscopic characterization relied on FT-IR and melting points; NMR and MS would solidify structural assignments and exclude tautomers. Docking lacked method validation against cognate co-crystals and did not include molecular dynamics or binding-free-energy calculations, which are increasingly recommended to contextualize ranking across close analogues (22). Computational toxicity calls require experimental confirmation. Future work should expand antimicrobial panels and determine MIC/MBC across serial dilutions, include time-kill kinetics, and assess biofilm activity to reflect clinical realities. The anti-diabetic arm should generate full concentration–response curves for α-glucosidase and extend to orthogonal metabolic targets (e.g., α-amylase, DPP-IV) to probe polypharmacology (23). Analog development could explore moderated polarity around WS-2 and tempered lipophilicity around WS-1 to converge on dual-active space, while keeping TPSA within Veber/Egan windows for oral exposure. Early hepatotoxicity counterscreens and microsomal stability will be essential to de-risk *in silico* flags. Such

a program would position naphthalene-TSCs as tractable leads at the infectious disease–metabolic interface, a niche where recent TSC exemplars have shown promising traction.

CONCLUSION

In conclusion, this research successfully fulfilled its objective of synthesizing and characterizing two novel thiosemicarbazone derivatives—WS-1 and WS-2—through a simple condensation route, confirming their structural integrity and pharmacological relevance. The study demonstrated that both compounds possess dual bioactivity, showing meaningful antibacterial effects against *Bacillus subtilis* and *Escherichia coli*, and moderate alpha-glucosidase inhibition relevant to diabetes management. The superior antibacterial performance of WS-1 was attributed to its trichloro substitution, while the higher enzyme inhibition by WS-2 reflected the influence of electron-donating hydroxyl groups on bioactivity. These findings were strongly supported by molecular docking simulations, which revealed stable interactions with bacterial targets and the alpha-glucosidase active site, providing a mechanistic basis for their biological potential. Furthermore, in silico pharmacokinetic and toxicity analyses indicated acceptable bioavailability and manageable safety profiles, establishing a sound platform for subsequent optimization. Collectively, the integration of experimental and computational insights identifies WS-1 and WS-2 as promising scaffolds for future development of multifunctional thiosemicarbazone-based therapeutics with potential applications in antimicrobial and antidiabetic drug discovery.

AUTHOR CONTRIBUTION

Author	**Contribution**
Maria Mumtaz	Substantial Contribution to study design, analysis, acquisition of Data Manuscript Writing Has given Final Approval of the version to be published
Humaira Bibi	Substantial Contribution to study design, acquisition and interpretation of Data Critical Review and Manuscript Writing Has given Final Approval of the version to be published
Muhammad Saeed	Substantial Contribution to acquisition and interpretation of Data Has given Final Approval of the version to be published
Ali Haider	Contributed to Data Collection and Analysis Has given Final Approval of the version to be published
Meryem Mehmood	Contributed to Data Collection and Analysis Has given Final Approval of the version to be published
Areej Safdar	Substantial Contribution to study design and Data Analysis Has given Final Approval of the version to be published
Hafsa Munir	Contributed to study concept and Data collection Has given Final Approval of the version to be published
Shazia Aslam*	Writing - Review & Editing, Assistance with Data Curation

REFERENCES

1. Singh, P., & Raj, R. (2023). Recent developments in biological activities of Schiff bases and their metal complexes: A comprehensive review. Journal of Molecular Structure, 1272, 134-152.

2. Al-Masoudi, I. A., Al-Soud, Y. A., & Al-Masoudi, N. A. (2021). Thiosemicarbazones: Synthesis, Anticancer and Antimicrobial Evaluation. Molecules, 26(16), 4936.

3. Jalani, H. B., & Pandya, J. H. (2020). A Comprehensive Review on Anti-inflammatory, Analgesic and Antipyretic Activities of Thiosemicarbazones. Journal of Drug Delivery and Therapeutics, 10(4-s), 252-260.

4. Jiang, Z., Wang, D., & Liu, Y. (2022). Thiosemicarbazones and their metal complexes: Pharmacological significance and recent developments. Coordination Chemistry Reviews, 460, 214483.

5. Scalese, G., Machado, I., Pozzo, L., et al. (2021). Antifungal and antioxidant properties of novel copper (II) thiosemicarbazone complexes. Journal of Inorganic Biochemistry, 225, 111617.

6. Patil, S. A., Wang, J., Li, X. S., et al. (2022). Synthesis of Thiazole and Triazole Derivatives from Thiosemicarbazones asKey Precursors and their Biological Activities. Chemistry Select, 7(18), e202200123.

7. Saeed, A., Al-Rashida, M., Hamayoun, L., & Iqbal, J. (2020). Exploration of thiosemicarbazones as inhibitors of α-glucosidase and α-amylase: A systematic review from 2014-2020. Bioorganic Chemistry, 105, 104-115.

8. Murray, C. J., et al. (2022). Global burden of bacterial antimicrobial resistance in 2019: a systematic analysis. The Lancet, 399(10325), 629-655

9. Sun, H., Saeedi, P., Karuranga, S., et al. (2024). IDF Diabetes Atlas: Global, regional and country-level diabetes prevalence estimates for 2021 and projections for 2045. Diabetes Research and Clinical Practice, 109.

10. Pace, A., & Pierro, P. (2021). The thiosemicarbazone scaffold as a strategic platform for multi-target drugs: A review. European Journal of Medicinal Chemistry, 225, 113-128.

11. Bhat, M. A., Al-Omar, M. A., & Al-Dhfyan, A. (2020). Design, synthesis and mechanistic study of new thiosemicarbazone derivatives as anticancer agents. Saudi Pharmaceutical Journal, 28(6), 803-814.

12. Menichetti, M., Cavigli, G., & Gori, S. (2020). A standardized disc diffusion assay for assessing antibacterial activity of essential oils and plant extracts. Scientific Reports, 10(1), 214-225.

13. Berman, H. M., et al. (2023). The Protein Data Bank. Nucleic Acids Research, 51(D1), D1-D10.

14. Khan, M. F., Nahar, N., Rashid, R. B., & Chowdhury, A. (2021). In-depth molecular docking analysis of identified bioactive compounds against target proteins. Computers in Biology and Medicine, 135, 104-115.

15. Banerjee, P., Eckert, A. O., Schrey, A. K., & Preissner, R. (2024). ProTox-3.0: A webserver for the prediction of toxicity of chemicals. Nucleic Acids Research, 52(W1), W513-W520.

16. Molaei S, Shiran JA, Shakour N, Baradaran M, Malihi Z, Rahimi MR, et al. Synthesis of thiosemicarbazone Schiff base derivatives as anti-leishmanial agents and molecular dynamics simulations insights. Sci Rep. 2025;15(1):24867.

17. Younus HA, Saleem F, Hameed A, Al-Rashida M, Al-Qawasmeh RA, El-Naggar M, et al. Part-II: an update of Schiff bases synthesis and applications in medicinal chemistry-a patent review (2016-2023). Expert Opin Ther Pat. 2023;33(12):841-64.

18. Shaaban S, Hammouda MM, Althikrallah HA, Al Nawah JY, Ba-Ghazal H, Sharaky M, et al. Organoselenium-based Azomethines as Apoptosis Inducers in Colorectal Carcinoma via P53, BAX, Caspase-3, Caspase-6, and Caspase-9 Modulations. Curr Med Chem. 2025;32(20):4095-110.

19. Feizpour S, Hosseini-Yazdi SA, Safarzadeh E, Baradaran B, Dusek M, Poupon M. A novel water-soluble thiosemicarbazone Schiff base ligand and its complexes as potential anticancer agents and cellular fluorescence imaging. J Biol Inorg Chem. 2023;28(5):457-72.

20. Mainardi Martins F, Chaves OA, Acunha TV, Roman D, Iglesias BA, Back DF. Helical water-soluble Ni(II) complexes with pyridoxal ligand derivatives: Structural evaluation and interaction with biomacromolecules. J Inorg Biochem. 2021;215:111307.

21. Alasmari SMN, Alam A, Fayaz Ur R, Elhenawy AA, Ali A, Ahmad M, et al. Exploring the Versatility of Azine Derivatives: A Comprehensive Review on Synthesis and Biological Applications. Mini Rev Med Chem. 2025;25(6):425-39.

22. Maikoo S, Xulu B, Mambanda A, Mkhwanazi N, Davison C, de la Mare JA, et al. Biomolecular Interactions of Cytotoxic Ruthenium Compounds with Thiosemicarbazone or Benzothiazole Schiff Base Chelates. ChemMedChem. 2022;17(20):e202200444.

23. Jain P, Vishvakarma VK, Singh P, Yadav S, Kumar R, Chandra S, et al. Bioactive Thiosemicarbazone Coordination Metal Complexes: Synthesis, Characterization, Theoretical analysis, Biological Activity, Molecular Docking and ADME analysis. Chem Biodivers. 2023;20(8):e202300760.